Toxicology Reports 1 (2014) 1076–1086

Contents lists available at ScienceDirect

Toxicology Reports

journal homepage: www.elsevier.com/locate/toxrep

Proapoptotic activity of aflatoxin B_1 and sterigmatocystin in HepG2 cells

Yang Liu, Ming Du, Genyi Zhang*

State Key Laboratory of Food Science and Technology, School of Food Science and Technology, Jiangnan University, 1800, Lihu Avenue, Wuxi 214122, Jiangsu Province, PR China

ARTICLE INFO

Article history:
Received 31 July 2014
Received in revised form 15 October 2014
Accepted 17 October 2014
Available online 29 October 2014

Keywords:
Aflatoxin B_1
Sterigmatocystin
Combinative toxicity
Apoptosis

ABSTRACT

Aflatoxin B_1 (AFB_1) and sterigmatocystin (ST) are two hepatocarcinogenic mycotoxins that are commonly coexisted in cereal grains, and their co-proapoptotic activity in HepG2 cells was studied. The values of IC_{50}, which is the dosage of mycotoxin resulting in a 50% cell growth inhibition measured by a sulforhodamine B (SRB) colorimetric assay, were 16.9 μM and 7.3 μM for AFB_1 and ST, respectively. Additively and dose-dependently, cell apoptosis-related toxicity endpoints of double strand DNA and ATP content were decreased while the intracellular ROS and mitochondria membrane permeability (MMP) were increased. Consistently, when cell cycle is arrest at G0/G1 or S phase by AFB_1 and/or ST, the experimental results from flow cytometry assay demonstrated that the rate of cell apoptosis and mitochondrial membrane potential were also additively increased and decreased, respectively, in a dose-dependent manner. Thus, the integrity of mitochondria (MMP and membrane potential) that is the central component of cell apoptosis is disrupted by AFB_1 and ST in an additive manner. With the immunocytochemistry analysis showing increased expression of apoptosis-related proteins of Bax, Caspase-3 and p53 and decreased expression of Bcl-2 protein, an additive nature of the co-proapoptotic activity of AFB_1 and ST was revealed.

1. Introduction

Aflatoxin (AF) is a class of mycotoxins mainly produced by *Aspergillus flavus* and *Aspergillus parasiticus*, and there are multiple types of aflatoxin including AFB_1, AFB_2, AFG_1 and AFG_2 with different structures and physiochemical properties [1]. Among all these types of aflatoxin, AFB_1 has shown to be the highest toxic agent [2] with its potent genotoxic, hepatocarcinogenic [3], and reproductive toxicity [4]. The formation of reactive AFB_1-epoxide by the action of cytochrome P450 enzymes is the central pathway to its genotoxicity [5]. Many animal studies confirmed its toxicity with a LD_{50} between 0.3 and 17.9 mg/kg varied by animal models. More importantly, the microorganisms from *Aspergillus* genus are widely present in the natural world, and AFB_1 contamination has been shown in many cereal grains such as corn [6] and rice [7], and it has become a serious food-borne hazard. Although numerous detection methods and technologies to eliminate AFB_1 from food ingredients have been developed, AFB_1 contamination is still a major challenge to food industry and public health since aflatoxin contamination in food chains can occur at any stage of food production, processing, transport and storage.

Co-exposure to multiple mycotoxins has become a public health concern since human body is rarely exposed to

Abbreviations: ATCC, American type culture collection; AFB_1, aflatoxin B_1; FCM, flow cytometry assay; ST, sterigmatocystin; SRB, sulforhodamine B; MMP, mitochondrial membrane permeability; PCA, principle component analysis; PI, propidium iodide.

* Corresponding author. Tel.: +86 0510 85328726.
E-mail address: genyiz@163.com (G. Zhang).

http://dx.doi.org/10.1016/j.toxrep.2014.10.016

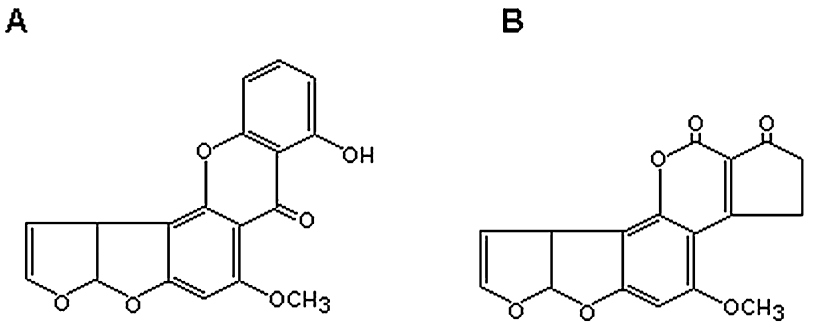

Fig. 1. Chemical structures of sterigmatocystin (A) and aflatoxin B_1 (B) sharing a common bisdihydrofuran moiety.

one type of mycotoxin, and some mycotoxin combinations might produce a synergistic toxicity. The combinative toxicity of AFB_1 with deoxynivalenol (DON) [8], T-2 [9], and fumonisin B_1 [10] have been reported, and additive or synergistic interaction have been discovered in some combinations. Sterigmatocystin (ST) and AFB_1 – structurally similar mycotoxin with a bisdihydrofuran moiety (Fig. 1), has similar toxicity to AFB_1 [11]. Both of them can inhibit ATP synthesis [12] and impair cell cycle [13]. ST is also a carcinogenic agent [14] and an adduct of 1,2-dihydro-2-(N(7)-guanyl)-1-hydroxysterigmatocystin can be formed through its reaction with DNA in an exo-ST-1,2-oxide structural form [15]. Regarding the coexistence of AFB_1 and ST, there have been reports that both of them are produced by the same species, such as *Emericella venezuelensis* [16] and *Emericella astellata* [17]. ST is also widely present in cereal grains of corn and food product of bread [18], and their coexistence was also detected in urine from a human study [19]. Thus, coexistence of AFB_1 and ST is present in nature and food chains. Although toxicities of AFB_1 [10] and ST [20] and their precursors [21] have been studied individually and comparatively, their combinative toxicity related to cell apoptosis has not been fully investigated, and it is worth of further investigation from a mechanistic point of view so that preventive or interventive measures can be developed to ameliorate their in vivo toxic effects. Due to the hepatocarcinogenic property of both AFB_1 and ST, the human hepatoma HepG2 cell was used as the cell model to investigate their co-proapoptotic activity and related mechanisms, and it is expected that the basic toxicity property and mechanism obtained from a model system might facilitate developing interventive measures to reduce their vivo toxicity to the body.

2. Materials and methods

2.1. Materials

Human hepatoma HepG2 cells lines were obtained from American Type Culture Collection (ATCC, Beijing, China). AFB_1 (purity ≥ 98%), ST (purity ≥ 98%), DMSO, sulforhodamine B (SRB), TCA, H33258, DCFH-DA, DCF, rhodamine 123, JC-1 dye, and calf thymus DNA were purchased from Sigma–Aldrich (Shanghai, China). Dulbecco's Modified Eagle Medium (DMEM), fetal bovine serum (FBS), trypsin, HBSS, and phosphate-buffered saline (PBS) were purchased from Gibco Life Technologies (Shanghai, China). ATP assay kit, Annexin V-FITC cell apoptosis assay kit, and mitochondria membrane potential assay kit were obtained from Beyotime Institute of Biotechnology (Shanghai, China). DAB was purchased from Genetech Inc. (Shanghai, China). All the antibodies for Caspase-3, p53, Bax and Bcl-2 were from Germany AbioB, LTM. (Shanghai, China).

2.2. Cell culture

HepG2 cells were cultured in DMEM medium containing FBS (10%), penicillin (100 units/mL) and streptomycin (100 μg/mL) under a humidified incubator with CO_2 (5%) and air (95%) at 37 °C. Every 5–7 days, the adherent cells were suspended after treatment with 1 mL of 0.25% trypsin–EDTA solution for 2–3 min at 37 °C, and then were subcultured at a 1:3 split ratio. The culture medium was changed every 2 days. Stocks of cells were routinely frozen and stored in liquid nitrogen. Cells with 15–20 passages were used for experiments to ensure cell line stability.

2.3. Determination of cell viability

The cell viability was measured by a sulforhodamine B colorimetric assay (SRB) [22]. Briefly, log phase HepG2 cells (200 μL) were seeded at a density of 3×10^4 cells/mL in a 96-well plate. After incubation for 24 h, culture medium containing AFB_1 or ST (dissolved in DMSO) was used to treat the cells for 24 or 48 h. Then, the cells were fixed by adding 100 μL cold (4 °C) trichloroacetic acid (TCA) solution (10% w/v) and incubated at 4 °C for 1 h, and then gently washed with deionized water four to five times. After the plate was air-dried, 100 μL SRB reagent (4 g/L) was added and incubated at room temperature for 30 min, then the plate was washed with 1% acetic acid four to five times and air-dried. The OD reading at 490 nm was carried out by adding 200 μL 10 mM Tris–HCl buffer (pH 7.4) to each well. Cell growth inhibition rate in percentage was calculated by comparing with the control sample (without AFB_1 and ST treatment).

2.4. Cytotoxicity endpoint measurement

HepG2 cells were seeded at a density of 5×10^4 cells/mL in a 96-well plate. After the seeded cells were incubated with AFB_1 or ST for 24 h and 48 h, cytotoxicity endpoints of ATP and DNA content, ROS and mitochondria membrane

permeability (MMP) were measured to reflect the toxic effect of AFB_1 and ST on HepG2 cells. Briefly, the double strand DNA content was measured using a H33258 reagent after cell lysis as described by Rage et al. [23]. Reactive oxygen species (ROS) were measured by oxidation of dihydrodichlorofluorescein to dichlorofluorescein as described in literature [24]. Mitochondria membrane permeability (MMP) was measured by the uptake and retention of rhodamine 123 as described by Rat et al. [25]. ATP content was measured using the assay kit as described by the assay manual.

2.5. Flow cytometry assay (FCM)

A FCM (Becton, Dickinson and Company, New Jersey, USA) was employed to examine the mitochondria membrane potential, cell cycle and apoptosis of HepG2 cell after treatment with AFB_1 and ST. The mitochondria membrane potential ($\Delta\Psi m$) is measured using the JC-1 dye as described by literature report [26] by differentiation of the energized and de-energized mitochondria based on the fluorescent color. The cell cycle analysis is based the propidium iodide (PI) dye that can bind double strand DNA [27], and the analysis protocol detailed in literature [28] was followed. The cell apoptosis was analyzed by employing staining reagent of PI and Annexin V-FITC as described by Vermes et al. [29].

2.6. Immunocytochemistry analysis of HepG2 cell apoptosis

In order to analyze the proapoptotic activity of AFB_1 and ST in HepG2 cells, the apoptotic signaling pathway was also analyzed by immunocytochemistry using apoptosis related markers of Bax, Bcl-2, p53, and Caspase-3. HepG2 cells at the logarithmic phase were collected at a density of 1×10^4 cells/mL. Sterile coverslips were added to a 24-well culture plate and then cell suspension was added to allow the cells seeded on the slips. After the cells become adherent, medium containing AFB_1, ST and their mixture was added (in triplicate). After 48 h incubation, the slips were removed and fixed in formalin for 20 min, and then air-dried at room temperature. The slips were then hydrated through a gradient of ethanol (two times, 1 min) – 95% ethanol (two times, 1 min) – 70% ethanol (one time, 1 min) – water washed out after 5 min. Endogenous peroxidase activity was blocked by adding100 μL hydrogen peroxide and incubating at room temperature for 15 min, then it was washed three times with PBS with 5 min interval. The fixed slips were then placed in a boiling antigen retrieval solution for 15 min, incubated for 15 min, cooled out after the power is turned off and washed three times (5 min interval) with PBS. Non-immune serum (100 μL) from the same source of secondary antibody was added on each slip, incubated at 37 °C for 20 min, then diluted serum (antibody) (50 μL) was added (Bax 1:300, Bcl-2 1:250, Caspase-3 1:200, p53 1:200) and incubated overnight at 4 °C. After incubation for 1 h at room temperature, the slips were washed with PBS three times (each time 5 min). The labeled secondary antibody (50 μL) was added per slip, incubated at 37 °C for 30 min, and washed with PBS three times (each time, 5 min). After this was done, DAB was added to each slip and observed under a microscope, the staining was terminated immediately by washing the residual DAB liquid with water when yellow particles appears. Hematoxylin was added to react for 30 s, then washed with water 5 min, and differentiated by hydrochloride alcohol for 1 s and washed for 10 min. The coverslips were then dehydrated through a gradient of ethanol: 70% ethanol (one time, 3 min) – 95% ethanol (two times, 3 min) – ethanol (one time, 3 min) – xylene (three times, 5 min). The air-dried coverslip was mounted on a glass slide using a silicone–urethane adhesive reagent [30]. Bax, Bcl-2 proteins were localized in the cytoplasm/nucleus showing brownish yellow. Caspase-3 protein positive results showed brown particles present in the cytoplasm with a blue nucleus. Brownish yellow nuclei indicate p53 protein positive results. Three horizons on each slide were selected to take pictures, and the mean optical density of positive area was calculated using image analysis software of Image-Pro Plus 6.0 (Media Cybernetics, Inc., Rockville, USA) based on the operation manual. Briefly, for each protein, its specific color at specific locations was clicked, and the total intensity at the positive area (with the same color in defined scope) was recorded and then the optical density (total intensity/area) was calculated automatically.

2.7. Statistic analysis

All the data were expressed as average with standard deviation. Probit analysis (StatsDirect Ltd., Cheshire, UK) was used to calculate the IC_{50} for AFB_1 and ST. The type of combinative toxicity is based on the method of Weber et al. [31] by comparing the measured cytotoxicity with the calculated toxicity that was obtained by adding the individual endpoint values at the same concentrations used in the combinative treatments, and the statistic difference between them (measured value and calculated value) was analyzed by unpaired *t*-test by SSPS 20.0 (IBM). If it is not statistically different at a significant level of $p < 0.05$, it is determined as additive toxicity. If it is different significantly, it would be synergistic (measured value > calculated value) or antagonistic (measured value < calculated value). For other comparisons between treatment and control groups, Student's *t*-test was used while paired *t*-test was applied when comparing different groups. In the meantime, the principle component analysis (PCA) of the endpoints was also conducted to cluster the endpoints.

3. Results and discussion

3.1. Cytotoxicity of AFB_1 and ST in HepG2 cells

For cytotoxicity analysis, the IC_{50} is one important parameter, and based on the dose-response relationship (Fig. 2) measured by a SRB method, the IC_{50} were analyzed to be 16.9 μM and 7.3 μM for AFB_1 and ST, respectively. For AFB_1, the cell growth was not affected significantly at low concentrations (<1 μM) while the cell was more sensitive to ST showing a linear inhibition of cell viability along its concentrations. Apparently, ST is more toxic than AFB_1 to

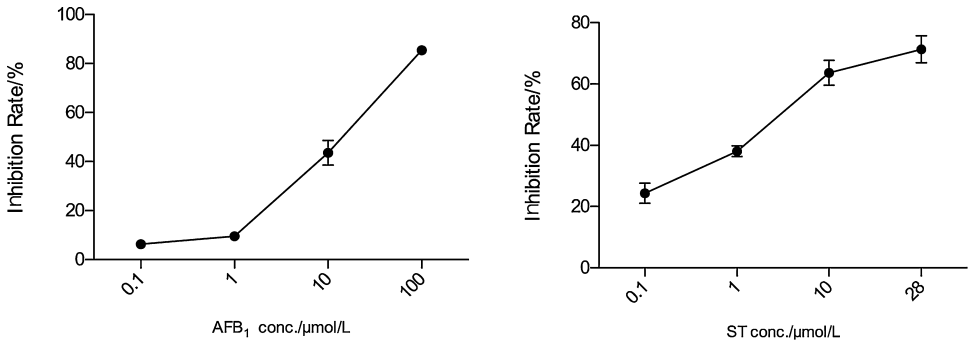

Fig. 2. The dose-response relationship of HepG2 cell viability affected by AFB_1 and ST.

HepG2 cells, and the low water solubility of ST is likely the reason since low water solubility makes it easy to diffuse into the cells. For AFB_1, its high value of IC_{50} is different from literature reports measured by MTT test [10], and this is likely due to different methods used to measure cell viability. SRB refers to the total protein in the cell [22] while MTT test is based on the enzyme activity of NAD(P)H-dependent cellular oxidoreductase [32], so there is possible discrepancy between the two methods, and the value of IC_{50} is likely dependent on the cell viability measurement method. Regarding different values of IC_{50} between AFB_1 and ST, there is a literature report that the IC_{50} of AFB_1 (10 μM) is greater than that of ST (3.7 μM) in human lung cancer cell line of A549 [10,33], which also showed that ST is more toxic than AFB_1. Another literature report [11] also showed noticeable difference between AFB_1 and ST in hormonal induction of tyrosine aminotransferase with different values of IC_{50} in a rat hepatoma cell line of H4-II-E.

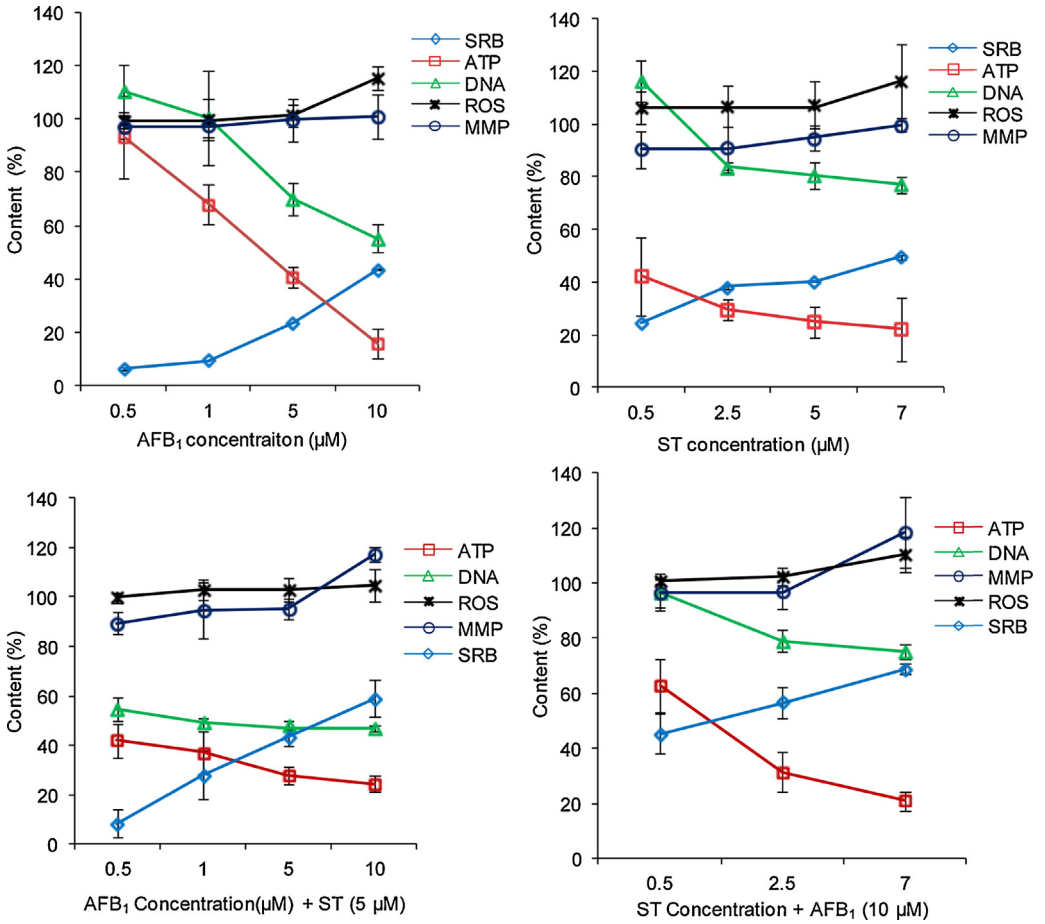

Fig. 3. The cytotoxicity endpoints after exposed to individual AFB_1 and ST and their combinations at different dosages. All the values were obtained by comparing to the control and expressed as percentage. SRB represents the cell growth inhibition rate.

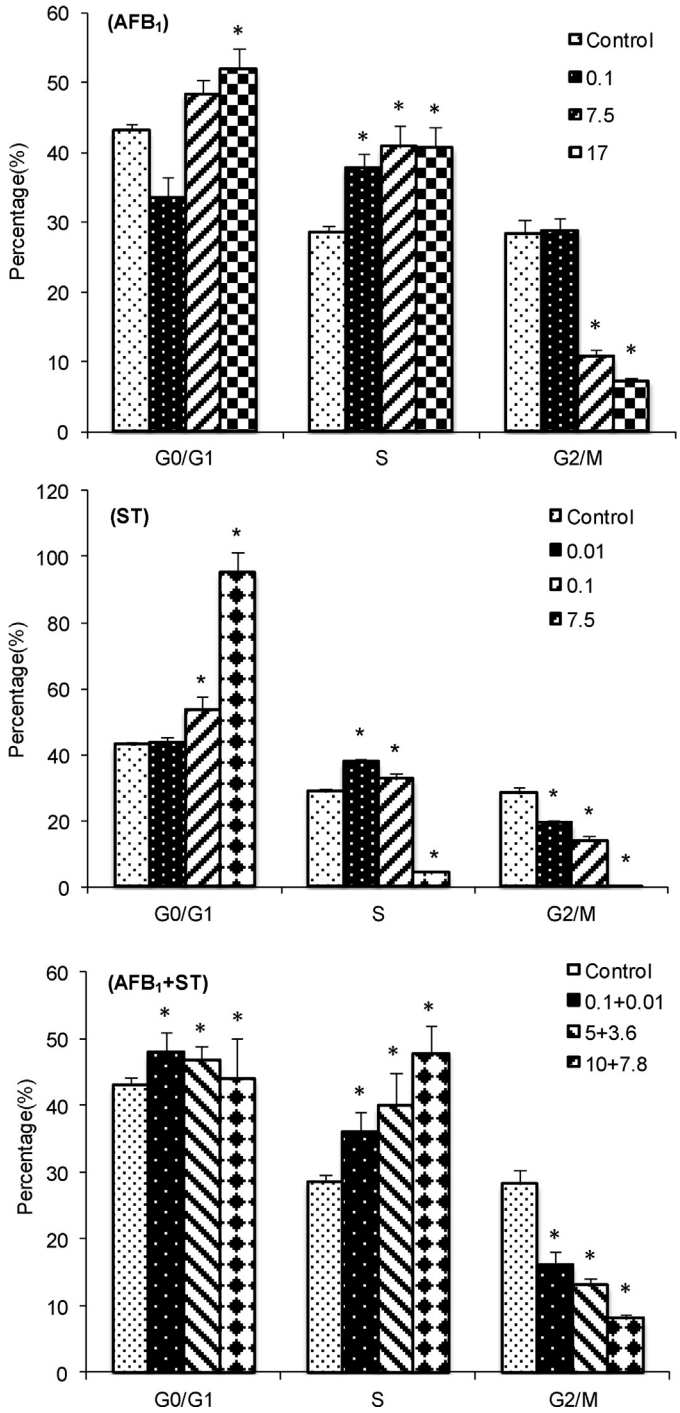

Fig. 4. The cell cycle distribution of HepG2 cells after exposed to AFB_1, ST and their combination (AFB_1 + ST). The legend represents the concentration (μmol/L) and combination. * indicates significant difference ($p < 0.05$) compared to the control.

The cytotoxicity endpoints of ROS, mitochondria membrane permeability (MMP), DNA and ATP content all showed cytotoxicity of AFB_1 and ST (Fig. 3) to HepG2 cells, and all the endpoints show similar trends when HepG2 cells were exposed to individual AFB_1 and ST or their combinations.

The contents of both ATP and DNA were decreased while the ROS and MMP were increased along the treatment concentrations. Comparatively, the decrease of ATP and DNA is more evident than the increase of ROS and MMP, and ST is more potent to decrease ATP content. However, no significant difference between the measured combinative

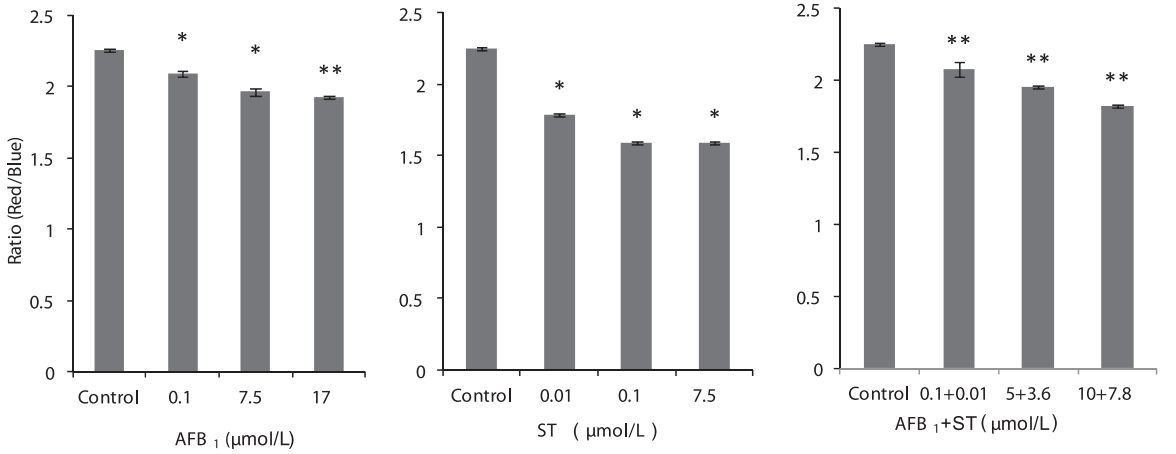

Fig. 5. The mitochondria membrane potential of HepG2 cells represented by the ratio of red (high potential) to blue (low potential) florescent when exposed to AFB_1 and ST. * $p < 0.05$, ** $p < 0.01$ (statistic analysis was compared to the control).

Table 1
Correlation analysis among all the endpoints (correlation coefficient *R* and *p* values).

	ATP	DNA	ROS	MMP
DNA	0.636			
	0.0108*			
ROS	−0.686	−0.162		
	0.0047*	0.564		
MMP	−0.294	−0.278	0.293	
	0.2867	0.315	0.289	
SRB	−0.695	−0.333	0.549	0.635
	0.004*	0.2254	0.034*	0.011*

* Statistically significant at $p < 0.05$.

toxicity and the calculated toxicity (by adding the values of each endpoint at corresponding concentrations used in their combinations) demonstrates an additive nature of their combinative cytotoxicity.

Correlation analysis on the relationship among all the endpoints showed that ATP is positively correlated to DNA content, but negatively correlated to ROS and SRB at a significant level. Both ROS and MMP are positively correlated to SRB (Table 1). Thus, decreased cell viability of HepG2 cells is likely caused by the production of ROS, increased MMP and decreased ATP and DNA when exposed to AFB_1 and ST. Consistently, the PCA analysis of these endpoints showed that three clusters can be differentiated: SRB is one cluster, DNA and ATP content is the second cluster, and the third cluster includes ROS and MMP. Considering the biochemical processes associated with mycotoxin exposure, the increased intracellular ROS is a common feature for AFB_1 or other mycotoxins [34]. The increased intracellular ROS might cause cross-linking of mitochondria membrane protein and to induce membrane permeability transition and increased MMP [35]. The increase of MMP would result in a decrease of mitochondrial membrane electrochemical potential and uncoupling ATP production from mitochondrial respiratory chain, which would lead to a reduction of ATP production. Experimentally, ATP is the most sensitive endpoint, and its reduction can be detected in a very early stage. Possibilities of ATP consumption (e.g., up-regulation of detoxification genes) to generate non-mitochondria ROS such as NADPH oxidase in response to toxic effect of AFB_1 and ST might be another pathway for the negative correlation between ATP and ROS contents.

Although double strand DNA, ATP, ROS content and MMP are generally considered as cytotoxicity endpoints, their intimate relationship with cell viability indicates they are also parameters related to cell death program, and these endpoints could also be called apoptosis-associated toxicity endpoints evidenced by literature reports on cell apoptosis under high level of ROS such as H_2O_2 [36] and MMP [37] as well double strand DNA breakage [38].

3.2. Cell cycle, mitochondria membrane potential and cell apoptosis

The toxicity endpoints not only reflect the biochemical phenomenon when the HepG2 cell is exposed to AFB_1 and ST, but also indicate occurred biological events in the exposed cells such as cell cycle arrest and cell apoptosis. Apparently, the cell cycle is the basis for cell growth, and when the cell cycle is arrested, the cellular apoptosis is likely the final fate for the cell unless the cells can be recovered through their detoxification system.

Table 2
Experiment design of AFB_1 and/or ST concentration.

Inhibition rate (%)	AFB_1 (μmol/L)	ST (μmol/L)	Combination	
			AFB_1 (μmol/L)	ST (μmol/L)
10	0.1	0.01	0.1	0.01
30	7.5	0.1	5	3.6
50	17	7.5	10	7.8

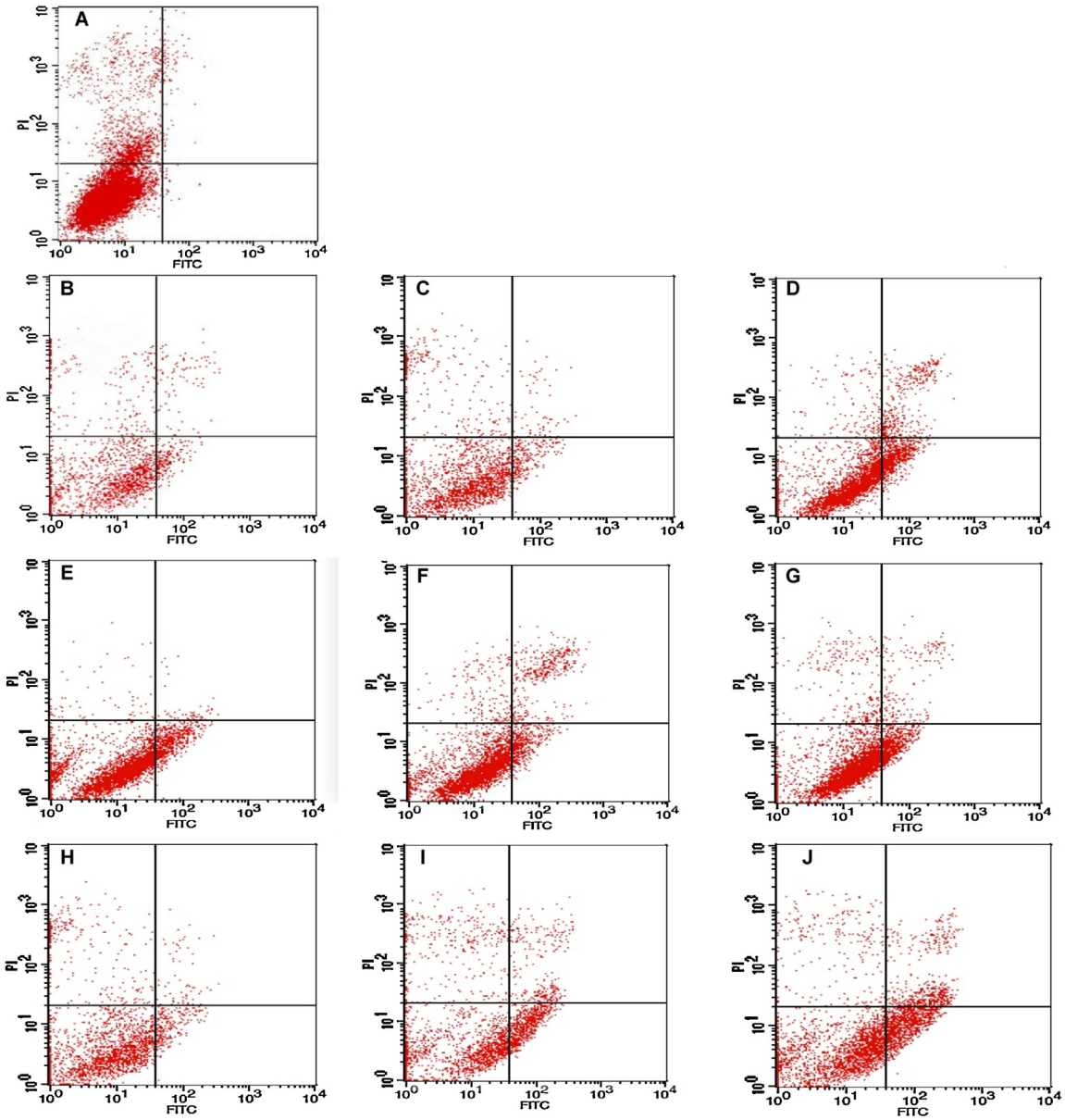

Fig. 6. (A): control. The changes of the apoptosis rate of HepG2 cell after exposed to AFB_1 (B–D: 0.1, 7.5, 17 μmol/L), ST (E–G: 0.01, 0.1, 7.5 μmol/L), and their combination of AFB_1 + ST (H–J: 0.1 + 0.01, 5 + 3.6, 10 + 7.8 μmol/L).

Cell cycle is divided into different phases of G0, G1, S, G2 and M in which G0 is the quiescent phase, and G1 is the gap between G0 and DNA synthesis (S phase) while G2 is the gap phase between DNA synthesis and mitotic phase (M) for cell division. Different phases of cell cycle are normally determined using FCM based on DNA content [28]. In the current experiment, equivalent toxicity dosages of AFB_1, ST and their combinations were first determined by measuring the SRB at different combinations, and the final result was tabulated in Table 2. It is noticed that the total amount of ST and AFB_1 in their combinative groups is somehow higher than their individual groups at equivalent SRB, especially for ST in the combinative groups. The reason for these combinations is likely due to their similar chemical structure with a common bisdihydrofuran moiety (Fig. 1) that might cause them to interfere with each other during their uptake by HepG2 cells.

The experimental results from FCM showed that both AFB_1 and ST caused cell cycle arrest at certain stages in a dose-dependent manner (Fig. 4). For AFB_1, most of cells are in the stage of S phase and least in the G2/M phase, indicating the cell arrest occurs at the phase of DNA synthesis, which is consistent with literature report [39]. For ST, most cells are stayed at the G0/G1 phase, indicating DNA synthesis is almost completely inhibited, especially at a high dose of ST, which is consistent with the decreased DNA content as shown above. For the combinations of AFB_1 and ST, most cells are stayed at G0/G1 and S phase, which is an

Table 3
The optic density of immunocytochemistry analysis of apoptosis related proteins of Bax and Bcl-2.

Protein	SRB	Optic density		
		AFB_1	ST	AFB_1 + ST
Bcl-2	10%	0.167 ± 0.022	0.236 ± 0.037	0.210 ± 0.045
	30%	0.165 ± 0.042	0.162 ± 0.042	0.171 ± 0.007
	50%	0.16 0 ± 0.030	0.120 ± 0.017	0.156 ± 0.034
	Control		0.213 ± 0.044	
Bax	10%	0.263 ± 0.04	0.329 ± 0.015	0.328 ± 0.047
	30%	0.475 ± 0.035	0.228 ± 0.034	0.245 ± 0.047
	50%	0.329 ± 0.062	0.185 ± 0.001	0.215 ± 0.051
	Control		0.239 ± 0.009	
Bax/Bcl-2	10%	1.57 ± 0.129	1.39 ± 0.117	1.56 ± 0.164
	30%	2.88 ± 0.092	1.40 ± 0.213	1.43 ± 0.137
	50%	2.05 ± 0.129	1.54 ± 0.141	1.37 ± 0.234
	Control		1.12 ± 0.187	

addition effect of AFB_1 and ST. Statistic analysis of the cell numbers at different stages after treatment by AFB_1 and ST and their combinations with equivalent toxicity (same SRB) did not show significant difference, indicating an additive effect of AFB_1 and ST on cell cycle arrest. As what has been shown previously that mitochondrion is highly associated with cell viability, especially the MMP. Here, the mitochondria membrane potential based on JC-1 dye [40] was further analyzed. The ratio between red (high potential) and blue (lower potential) florescent intensity reflects the mitochondria functionality in HepG2 cells affected by AFB_1 and ST (Fig. 5). Apparently, all the treatment led to a transition from red to blue florescent indicating decreased membrane potential in a dose-dependent manner. The fact that the combination of AFB_1 and ST did not show significant difference with the other individual groups at the same toxicity level showed additive effect of AFB_1 and ST on the mitochondria membrane potential. The decreased mitochondria membrane potential, as the biomarker of oxidative stress [41], is a direct result of increased MMP [42], which is consistent with the cytotoxicity endpoint results of increased ROS and MMP.

Mitochondria is the central player in cell apoptosis [43], and a decreased mitochondria membrane potential as well as increased membrane permeability would result in a release of proteins such as cytochrome c to activate caspase cascade and programmed cell death [44]. Thus, the apoptosis of HepG2 cell upon exposing to AFB_1 and ST was studied by FCM employing double staining reagents of propidium iodide (PI) and Annexin V labeled by fluorescein of isothiocyanatc (FITC) (green fluorescence) that can discriminate intact cells ($FITC^-/PI^-$) from apoptotic ($FITC^+/PI^-$) or necrotic cells ($FITC^+/PI^+$). The viable cell is present in the lower left quadrants (LLQ) of the panels while non-viable, necrotic cells are shown in the upper right quadrants (URQ), and the apoptotic cells are shown in the lower right quadrants (LRQ). The experimental results (Fig. 6) showed that most of the cells in the control sample (Fig. 6A) are present in the LLQ regions, and for samples treated by AFB_1 (Fig. 6B–D) and the combinations of AFB_1 and ST (Fig. 6H–J), the cell number in the LRQ regions increased in a dose-dependent manner. For ST treatment (Fig. 6E–G), the cell apoptosis occurs even at a very low concentration. With the trend of more cells present in the separation region between URQ and LRQ as the increase of cell number in LRQ regions (more evident in the group of AFB_1 + ST), the cells in the separation region might be regarded as apoptotic cells in their late stages. Thus, the total apoptotic cells include the cells at LRQ and those in the separation region of URQ and LRQ, and when taking them together (Fig. 7), all the treatments induced apoptosis of HepG2 cells. Although the apoptosis rate is increased along the concentration of the mycotoxins (except ST), no significant difference was found among groups (paired *t*-test) with equivalent toxicity indicating an additive nature of AFB_1 and ST on cell apoptosis.

3.3. Immunocytochemistry analysis of HepG2 apoptosis

FCM analysis by employing many different DNA staining dyes clearly showed cell cycle arrest, decreased mitochondria membrane potential, and cell apoptosis. In order to further confirm these results, the examination of apoptosis related proteins was carried out. Bax and Bcl-2 as the early regulator of cell apoptosis and cytochrome c release [45], Caspase-3 as the hallmark of apoptosis [46], and p53 as the regulator of cytochrome c release from mitochondria [47] were chosen as the representative proteins to

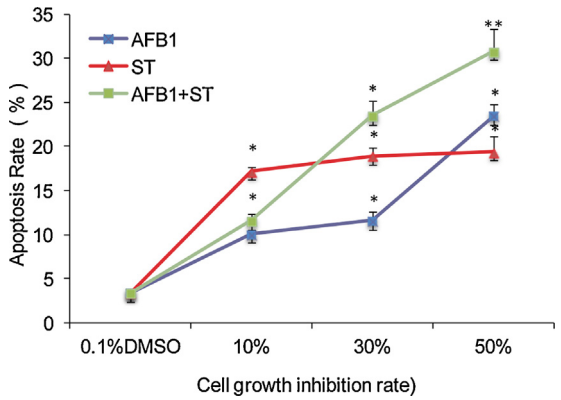

Fig. 7. The apoptosis rate of HepG2 cell induced by AFB_1 and ST as well as their combinations. The *x*-axis is the corresponding dosage that can induce the labeled cell viability inhibition. 0.1% DMSO is the control.

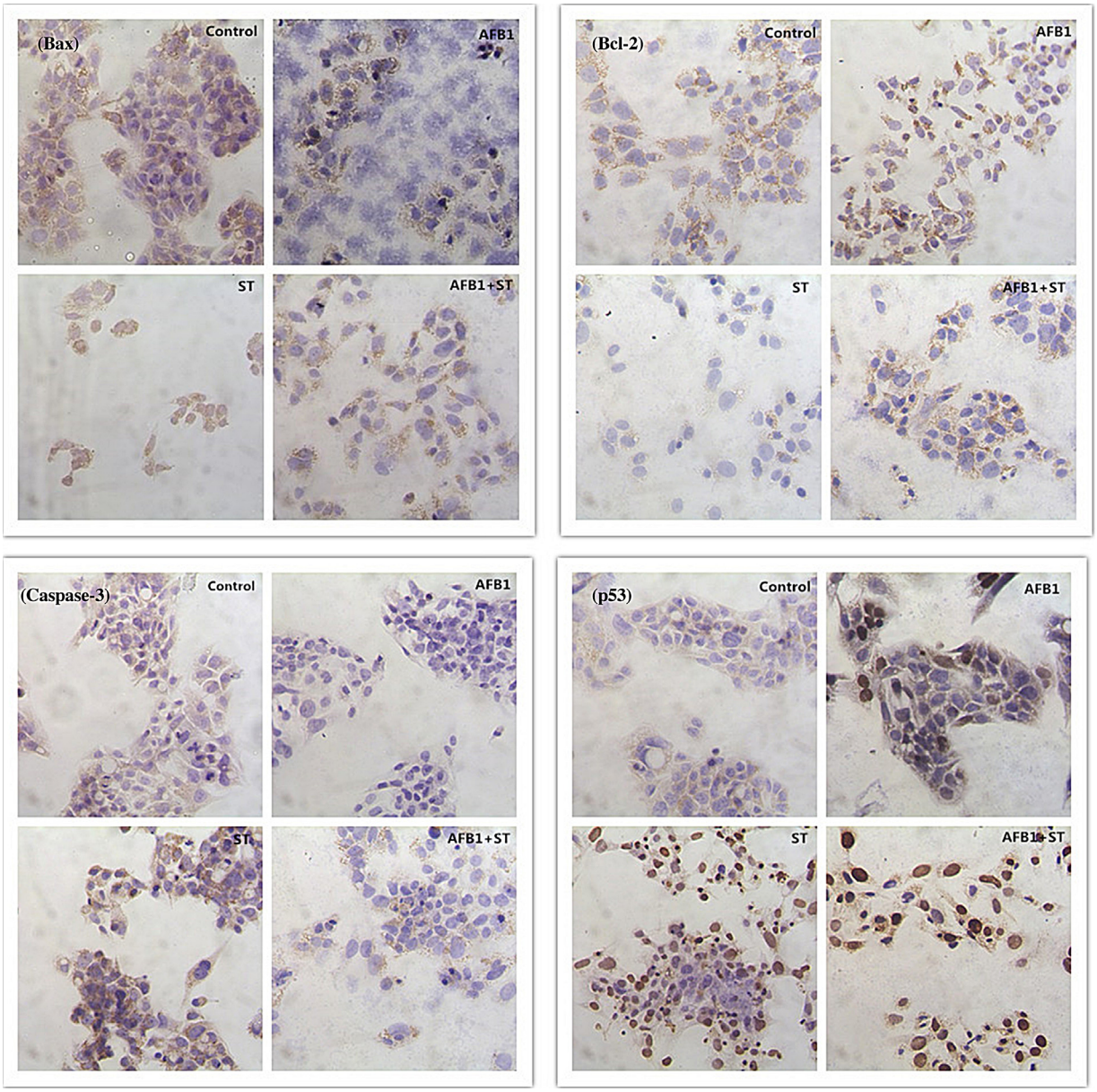

Fig. 8. Immunocytochemistry study on the expressions of apoptosis related proteins of Bax (top-left), Bcl-2 (top-right), Caspase-3 (bottom-left), and p53 (bottom-right) at a treatment dosage leading to 50% cell viability for all the groups was presented. (For interpretation of the references to color in text, the reader is referred to the web version of this article.)

analyze cell apoptosis upon exposed to AFB_1, ST and their combinations. Immunocytochemistry was selected as the method since the distribution of apoptosis-related proteins have different locations in the cell, and the analysis of these proteins in a cell context can be used to validate the event of cell apoptosis as well as to observe morphological changes of cells upon exposure to mycotoxins. However, the optical density of the proteins obtained though imaging analysis can only be used as a reference reflecting the trend of changes. In another word, the immunocytochemistry analysis is considered as a semi-quantitative method to evaluate the relative changes of protein expressions.

Mitochondria is an important player in cell apoptosis [45] with its apoptosis-associated BCL2 family proteins including Bax and Bcl-2. Bax promotes the release of cytochrome c [48] that is important to the activation of caspase cascade [49] while Bcl-2 is anti-apoptotic by regulating the activity of Bax. In normal cells, there exists a balance between these pro- and anti-apoptotic proteins, and a disruption of this balance often results in some pathological conditions such as human autosomal-dominant polycystic kidney disease with down-regulated Bcl-2 [50]. Thus the ratio of Bax and Bcl-2 might be more important to evaluate cell Apoptosis [51]. In the current investigation,

Bcl-2 showed a dose-dependent decrease of its content, and Bax, except the 10% dosage with an increased content, also showed a decreased expression compared to the control (Table 3). It looks like that both Bax and Bcl-2 from imaging analysis showed a decrease as the increase of the concentration of AFB_1 and ST, but the ratio of Bax and Bcl-2 with a value from 1.37 to 2.88 in the treatment group is higher than the control group of 1.12, supporting the pro-apoptotic function of Bax and Bcl-2 to HepG2 cells upon exposed to mycotoxins. The decreased signal of Bax at high level exposure to mycotoxin is probably due to the degradation of Bax since the induced cytochrome c release by Bax is the earliest event occurred during cell apoptosis, and with high rate of cell apoptosis at high dosage (more dead cells at the later phase of apoptosis), the Bax protein might have been degraded by the caspase cascade leading to a decreased signal of Bax after 2-days treatment. As for Bcl-2, the decreased signal along the dosage might be caused by a lower expression of Bcl-2 as what has been shown in the literature [52]. The immunocytochemistry image (Fig. 8) at 50% cell growth inhibition showed the brownish color of Bax and Bcl-2 in the cytosol with a blue nucleus confirmed the expression of both Bax and Bcl-2 proteins.

The occurrence of cell apoptosis is also supported by immunocytochemistry study of other apoptosis protein of Caspase-3 and p53 (Fig. 8). Compared to the control, noticeable increase of protein signals (brown color in cytosol) was shown for Caspase-3. Specifically, ST treatment showed increased optic density as the increase of dosage, but AFB_1 showed an increase from 10% to 30% SRB, and decreased signal from 30% to 50% SRB, and the combinative pattern is more close to AFB_1. For p53, the dose-optic density (expressed in nucleus) relationship showed a better trend as the increase of dosage for all the treatments, which indicates the involvement of p53 in the process of cell apoptosis. Considering the increased MMP and decreased membrane potential of mitochondria, and literature report [53], the process of apoptosis of HepG2 cells upon exposure to mycotoxins is likely a p53-dependent intrinsic process.

4. Conclusion

The co-proapoptotic cytotoxicity of AFB_1 and ST has been examined from apoptosis associated endpoints, cell cycle arrest, mitochondria integrity, and apoptosis related proteins. Due to the additive nature of AFB_1 and ST to cytotoxicity endpoints, cell cycle arrest distribution, apoptosis rate and membrane potential of mitochondria, AFB_1 and ST might additively promote the apoptosis of HepG2 cells. Although there have been many methods to reduce the level of mycotoxin contamination in food products or ingredients through physical, chemical or biological methods, consumption of mycotoxin-contaminated foods might be inevitable, especially in regions with high growth of mycotoxin-producing fungi, and mechanism-based preventive or interventive measure to reduce the in vivo toxicity of mycotoxin might be one strategy worth of further investigating. The current study showed that the mitochondria in the cell is one of the targets of AFB_1 and ST, which indicates some mitochondria-protective functional component might be used to protect the integrity of cells. Actually, there have been related reports such as the mitochondria-target functional peptide that has been used as neuroprotective agents [54] and antioxidant functional compounds to reduce the toxicity of mycotoxins [55]. Additionally, the additive effect of AFB_1 and ST combinations on cell apoptosis also provides scientific basis for food safety regulations to reduce the potential health risk associated with additive toxicity of coexisted mycotoxins in feeds and foods.

Conflict of interest

The authors declare no conflict of financial interest.

Transparency document

The Transparency document associated with this article can be found in the online version.

Acknowledgement

The current study is supported by the special fund for Agro-scientific Research in the Public Interest (Grant 201203069).

References

[1] L.V. Roze, S.Y. Hong, J.E. Linz, Aflatoxin biosynthesis: current frontiers, Annu. Rev. Food Sci. Technol. 4 (2013) 293–311.
[2] J.S. Wang, J.D. Groopman, DNA damage by mycotoxins, Mutat. Res. 424 (1–2) (1999) 167–181.
[3] M.C. Kew, Aflatoxins as a cause of hepatocellular carcinoma, J. Gastrointestin. Liver Dis. 22 (3) (2013) 305–310.
[4] C. Supriya, B.P. Girish, P.S. Reddy, Aflatoxin B1-induced reproductive toxicity in male rats: possible mechanism of action, Int. J. Toxicol. 33 (3) (2014) 155–161.
[5] C.A. de Oliveira, P.M. Germano, Aflatoxins: current concepts on mechanisms of toxicity and their involvement in the etiology of hepatocellular carcinoma, Rev. Saude Publica 31 (4) (1997) 417–424.
[6] N. Pande, J. Saxena, H. Pandey, Natural occurrence of mycotoxins in some cereals, Mycoses 33 (3) (1990) 126–128.
[7] K. Tanaka, Y. Sago, Y. Zheng, H. Nakagawa, M. Kushiro, Mycotoxins in rice, Int. J. Food Microbiol. 119 (1–2) (2007) 59–66.
[8] C.-H. He, Y.-H. Fan, Y. Wang, C.-Y. Huang, X.-C. Wang, H.-B. Zhang, The individual and combined effects of deoxynivalenol and aflatoxin B1 on primary hepatocytes of *Cyprinus carpio*, Int. J. Mol. Sci. 11 (2010) 3760–3768.
[9] C. McKean, L. Tang, M. Billam, M. Tang, C.W. Theodorakis, R.J. Kendall, J.S. Wang, Comparative acute and combinative toxicity of aflatoxin B1 and T-2 toxin in animals and immortalized human cell lines, J. Appl. Toxicol. 26 (2) (2006) 139–147.
[10] C. McKean, L. Tang, M. Tang, M. Billam, Z. Wang, C.W. Theodorakis, R.J. Kendall, J.S. Wang, Comparative acute and combinative toxicity of aflatoxin B1 and fumonisin B1 in animals and human cells, Food Chem. Toxicol. 44 (6) (2006) 868–876.
[11] N. Horikoshi, F. Tashiro, N. Tanaka, Y. Ueno, Modulation of hormonal induction of tyrosine aminotransferase and glucocorticoid receptors by aflatoxin B1 and sterigmatocystin in Reuber hepatoma cells, Cancer Res. 48 (18) (1988) 5188–5192.
[12] K. Kawai, T. Nakamaru, Y. Nozawa, Y. Maebayashi, M. Yamazaki, S. Natori, Inhibitory effect of sterigmatocystin and 5,6-dimethoxysterigmatocystin on ATP synthesis in mitochondria, Appl. Environ. Microbiol. 48 (5) (1984) 1001–1003.
[13] S. Huang, J. Wang, L. Xing, H. Shen, X. Yan, J. Wang, X. Zhang, Impairment of cell cycle progression by sterigmatocystin in human pulmonary cells in vitro, Food Chem. Toxicol. 66 (2014) 89–95.
[14] I.F.H. Purchase, J.J. van der Watt, Carcinogenicity of sterigmatocystin, Food Cosmet. Toxicol. 8 (3) (1970) 289–295.
[15] J.M. Essigmann, L.J. Barker, K.W. Fowler, M.A. Francisco, V.N. Reinhold, G.N. Wogan, Sterigmatocystin-DNA interactions: identification

of a major adduct formed after metabolic activation in vitro, Proc. Natl. Acad. Sci. U. S. A. 76 (1) (1979) 179–183.
[16] J.C. Frisvad, R.A. Samson, *Emericella venezuelensis*, a new species with stellate ascospores producing sterigmatocystin and aflatoxin B1, Syst. Appl. Microbiol. 27 (6) (2004) 672–680.
[17] J.C. Frisvad, R.A. Samson, J. Smedsgaard, *Emericella astellata*, a new producer of aflatoxin B, B and sterigmatocystin, Lett. Appl. Microbiol. 38 (5) (2004) 440–445.
[18] A. Versilovskis, S. De Saeger, Sterigmatocystin: occurrence in foodstuffs and analytical methods—an overview, Mol. Nutr. Food Res. 54 (1) (2010) 136–147.
[19] C. Hutanasu, C. Sfarti, A. Trifan, C. Cojocariu, A. Spac, M. Apostu, L. Miron, V. Dorneanu, C. Stanciu, High blood and urine concentration of hepatotoxic mycotoxins (aflatoxin B1, sterigmatocystin) in patients with liver cirrhosis, Rev. Med. Chir. Soc. Med. Nat. Iasi 113 (1) (2009) 59–63.
[20] N. Anninou, E. Chatzaki, F. Papachristou, M. Pitiakoudis, C. Simopoulos, Mycotoxins' activity at toxic and sub-toxic concentrations: differential cytotoxic and genotoxic effects of single and combined administration of sterigmatocystin, ochratoxin a and citrinin on the hepatocellular cancer cell line Hep3B, Int. J. Environ. Res. Public Health 11 (2014) 1855–1872.
[21] D. Jaksic, O. Puel, C. Canlet, N. Kopjar, I. Kosalec, M.S. Klaric, Cytotoxicity and genotoxicity of versicolorins and 5-methoxysterigmatocystin in A549 cells, Arch. Toxicol. 86 (10) (2012) 1583–1591.
[22] V. Vichai, K. Kirtikara, Sulforhodamine B colorimetric assay for cytotoxicity screening, Nat. Protoc. 1 (3) (2006) 1112–1116.
[23] R. Rage, J. Mitchen, G. Wilding, DNA fluorometric assay in 96-well tissue culture plates using Hoechst 33258 after cell lysis by freezing in distilled water, Anal. Biochem. 191 (1) (1990) 31–34.
[24] B. Yerushalmi, R. Dahl, M.W. Devereaux, E. Gumpricht, R.J. Sokol, Bile acid-induced rat hepatocyte apoptosis is inhibited by antioxidants and blockers of the mitochondrial permeability transition, Hepatology 33 (3) (2001) 616–626.
[25] P. Rat, C. Korwin-Zmijowska, J.M. Warnet, M. Adolphe, New in vitro fluorimetric microtitration assays for toxicological screening of drugs, Cell Biol. Toxicol. 10 (5–6) (1994) 329–337.
[26] A. Perelman, C. Wachtel, M. Cohen, S. Haupt, H. Shapiro, A. Tzur, JC-1: alternative excitation wavelengths facilitate mitochondrial membrane potential cytometry, Cell Death Dis. 2012 (22) (2012) 171.
[27] A. Krishan, Rapid flow cytofluorometric analysis of mammalian cell cycle by propidium iodide staining, J. Cell Biol. 66 (1) (1975) 188–193.
[28] P. Pozarowski, Z. Darzynkiewicz, Analysis of cell cycle by flow cytometry, in: A.H. Schönthal (Ed.), Methods in Molecular Biology, vol. 281, Humana Press Inc., Totowa, NJ, 2004, pp. 310–311.
[29] I. Vermes, C. Haanen, H. Steffens-Nakken, C. Reutelingsperger, A novel assay for apoptosis. Flow cytometric detection of phosphatidylserine expression on early apoptotic cells using fluorescein labelled Annexin V, J. Immunol. Methods 184 (1) (1995) 39–51.
[30] S. Matsunaga, Q. Xie, M. Kumano-Kuramochi, S. Komba, S. Machida, Silicone–urethane adhesive for improved coverslip mounting and leak-free preparation of living cell observation chambers, Biotechniques 46 (3) (2009) 225–227.
[31] F. Weber, R. Freudinger, G. Schwerdt, M. Gekle, A rapid screening method to test apoptotic synergisms of ochratoxin A with other nephrotoxic substances, Toxicol. In Vitro 19 (1) (2005) 135–143.
[32] T. Mosmann, Rapid colorimetric assay for cellular growth and survival: application to proliferation and cytotoxicity assays, J. Immunol. Methods 65 (1983) 55–63.
[33] J. Bünger, G. Westphal, A. Mönnich, B. Hinnendahl, E. Hallier, M. Müller, Cytotoxicity of occupationally and environmentally relevant mycotoxins, Toxicology 202 (3) (2004) 199–211.
[34] H.M. Shen, C.Y. Shi, Y. Shen, C.N. Ong, Detection of elevated reactive oxygen species level in cultured rat hepatocytes treated with aflatoxin B1, Free Radic. Biol. Med. 21 (2) (1996) 139–146.
[35] T. Kanno, E.E. Sato, S. Muranaka, H. Fujita, T. Fujiwara, T. Utsumi, M. Inoue, K. Utsumi, Oxidative stress underlies the mechanism for Ca(2+)-induced permeability transition of mitochondria, Free Radic. Res. 38 (1) (2004) 27–35.
[36] M. Pallardy, M. Perrin-Wolff, A. Biola, Cellular stress and apoptosis, Toxicol. In Vitro 11 (5) (1997) 573–578.
[37] J.-K. Ko, K.-H. Choi, Z. Pan, P. Lin, N. Weisleder, C.-W. Kim, J. Ma, The tail-anchoring domain of Bfl1 and HCCS1 targets mitochondrial membrane permeability to induce apoptosis, J. Cell Sci. 120 (16) (2007) 2912–2923.
[38] M. Nigro, G. Frenzilli, V. Scarcelli, S. Gorbi, F. Regoli, Induction of DNA strand breakage and apoptosis in the eel *Anguilla anguilla*, Mar. Environ. Res. 54 (3–5) (2002) 517–520.
[39] R. Ricordy, G. Gensabella, E. Cacci, G. Augusti-Tocco, Impairment of cell cycle progression by aflatoxin B1 in human cell lines, Mutagenesis 17 (3) (2002) 241–249.
[40] S. Salvioli, A. Ardizzoni, C. Franceschi, A. Cossarizza, JC-1, but not DiOC6(3) or rhodamine 123, is a reliable fluorescent probe to assess delta psi changes in intact cells: implications for studies on mitochondrial functionality during apoptosis, FEBS Lett. 411 (1) (1997) 77–82.
[41] M. Vayssier-Taussat, S.E. Kreps, C. Adrie, J. Dall'Ava, D. Christiani, B.S. Polla, Mitochondrial membrane potential: a novel biomarker of oxidative environmental stress, Environ. Health Perspect. 110 (3) (2002) 301–305.
[42] Y. Tsujimoto, S. Shimizu, Role of the mitochondrial membrane permeability transition in cell death, Apoptosis 12 (5) (2007) 835–840.
[43] C. Wang, R.J. Youle, The role of mitochondria in apoptosis*, Annu. Rev. Genet. 43 (2009) 95–118, http://dx.doi.org/10.1146/annurev-genet-102108-134850.
[44] J.C. Martinou, R.J. Youle, Mitochondria in apoptosis: Bcl-2 family members and mitochondrial dynamics, Dev. Cell 21 (1) (2011) 92–101.
[45] R.J. Youle, M. Karbowski, Mitochondrial fission in apoptosis, Nat. Rev. Mol. Cell Biol. 6 (8) (2005) 657–663.
[46] A.G. Porter, R.U. Janicke, Emerging roles of caspase-3 in apoptosis, Cell Death Differ. 6 (2) (1999) 99–104.
[47] M. Schuler, E. Bossy-Wetzel, J.C. Goldstein, P. Fitzgerald, D.R. Green, p53 induces apoptosis by caspase activation through mitochondrial cytochrome c release, J. Biol. Chem. 275 (10) (2000) 7337–7342.
[48] E. Er, L. Oliver, P.F. Cartron, P. Juin, S. Manon, F.M. Vallette, Mitochondria as the target of the pro-apoptotic protein Bax, Biochim. Biophys. Acta 1757 (9–10) (2006) 1301–1311 (Epub 2006 May 27).
[49] E.A. Slee, M.T. Harte, R.M. Kluck, B.B. Wolf, C.A. Casiano, D.D. Newmeyer, H.G. Wang, J.C. Reed, D.W. Nicholson, E.S. Alnemri, D.R. Green, S.J. Martin, Ordering the cytochrome c-initiated caspase cascade: hierarchical activation of caspases-2, -3, -6, -7, -8, and -10 in a caspase-9-dependent manner, J. Cell Biol. 144 (2) (1999) 281–292.
[50] T. Ecder, V.Y. Melnikov, M. Stanley, D. Korular, M.S. Lucia, R.W. Schrier, C.L. Edelstein, Caspases, Bcl-2 proteins and apoptosis in autosomal-dominant polycystic kidney disease, Kidney Int. 61 (4) (2002) 1220–1230.
[51] S. Salakou, D. Kardamakis, A.C. Tsamandas, V. Zolota, E. Apostolakis, V. Tzelepi, P. Papathanasopoulos, D.S. Bonikos, T. Papapetropoulos, T. Petsas, D. Dougenis, Increased Bax/Bcl-2 ratio up-regulates caspase-3 and increases apoptosis in the thymus of patients with myasthenia gravis, In Vivo 21 (1) (2007) 123–132.
[52] S.A. Sakinah, S.T. Handayani, L.P. Hawariah, Zerumbone induced apoptosis in liver cancer cells via modulation of Bax/Bcl-2 ratio, Cancer Cell Int. 7 (2007) 4.
[53] S. Fulda, K.M. Debatin, Extrinsic versus intrinsic apoptosis pathways in anticancer chemotherapy, Oncogene 25 (34) (2006) 4798–4811.
[54] H. Szeto, Mitochondria-targeted peptide antioxidants: novel neuroprotective agents, AAPS J. 8 (3) (2006) E521–E531.
[55] F. Galvano, A. Piva, A. Ritieni, G. Galvano, Dietary strategies to counteract the effects of mycotoxins: a review, J. Food Prot. 64 (1) (2001) 120–131.